

A bright γ -ray flare from the blazar B2 1215+30 detected by VERITAS and Fermi-LAT

Floriana Zefi*

Laboratoire Leprince-Ringuet, École Polytechnique, CNRS/IN2P3, 91128 Palaiseau, France

E-mail: floriana.zefi@llr.in2p3.fr

Reshmi Mukherjee for the VERITAS Collaboration

Barnard College, Columbia University, New York

E-mail: muk@astro.columbia.edu

Stephen Fegan, Berrie Giebels, Deirdre Horan

Laboratoire Leprince-Ringuet, École Polytechnique, CNRS/IN2P3, 91128 Palaiseau, France

We report on evidence of simultaneous γ -ray flaring from the BL Lac source B2 1215+30, detected by VERITAS ($E > 100$ GeV) and the *Fermi* Large Area Telescope (100 MeV $< E < 100$ GeV). The source was observed by VERITAS during an exceptional flaring state in 2014 February 08. Investigations of flux variability in the energy range covered by *Fermi*-LAT, show that the GeV flare occurred contemporaneously with the TeV flare. From the variability time scale we constrain the size of the emission region and derive a limit on the Doppler factor of the relativistic jet of B2 1215+30.

*The 34th International Cosmic Ray Conference,
30 July- 6 August, 2015
The Hague, The Netherlands*

*Speaker.

1. Introduction

B2 1215+30 (also known as ON 325 or 1ES 1215+303) was first detected as a radio source in the Bologna Northern Cross telescope survey conducted at 408 MHz [1]. In 2011, MAGIC discovered very-high-energy (VHE; $E > 100$ GeV) γ -ray emission from this source for the first time after an optical outburst was reported from the KVA telescope [2]. It was subsequently detected by VERITAS in 2012, when the source showed variability on time scales longer than months [3]. B2 1215+30 is classified as a bright intermediate-frequency-peaked BL Lac object (IBL) based on the position of the high energy peak in its spectral energy distribution (SED) [4]. The distance to this source is uncertain, with two different redshift values quoted in the literature, $z = 0.130$ [5] and $z = 0.237$ [6].

BL Lac objects are blazars, belonging to a subclass of Active Galactic Nuclei (AGN) with their relativistic jets pointing very close to the observer's line-of-sight. These objects are characterized by rapid, high-amplitude and broadband variability across the electromagnetic spectrum [7]. They also have featureless optical/UV spectra with very weak or no emission lines. The overall SED of blazars appears double-peaked with two distinct, broad components. The low-energy component with the maximum νF_ν peak from radio to UV/X-rays, is attributed to synchrotron emission from ultra-relativistic electrons in the jet magnetic field. The origin of the higher-energy peak may be due to either leptonic or hadronic processes. In the leptonic scenario, the emission is commonly believed to be the result of inverse-Compton scattering of seed photons off the same synchrotron-producing electrons in the jet. The source of the seed photons in this model could be either the synchrotron photons themselves, or photons from another external source.

The VERITAS imaging atmospheric-Cherenkov telescope array detected a massive γ -ray flare from the B2 1215+30 on 2014 February 08 during routine monitoring observations of the nearby blazar 1ES 1218+304. In this paper we describe and compare the long-term observations of the source taken by VERITAS (TeV energies), Fermi-LAT (GeV energies) and *Swift*-XRT (X-ray energies) from 2014 January to 2014 May. Using the variability time scale, we derive a lower limit on the Doppler factor of the emission region.

This proceedings is organized as follows: Sections 2, 3 and 4 describe the *Fermi*-LAT, VERITAS and *Swift*-XRT observations and analysis, respectively. Section 5 is dedicated to describing the Doppler factor calculation using the variability time scale derived from the *Fermi*-LAT data. Section 6 contains a short summary and the conclusions. In this work we assume a Friedmann universe with $H_0 = 73 \text{ km s}^{-1} \text{ Mpc}^{-1}$, $\Omega_m = 0.27$ and $\Omega_\lambda = 0.73$. All distance-dependent quantities for B2 1215+30 are calculated assuming a redshift of $z = 0.130$ ($d_L = 592 \text{ Mpc}$).

2. Fermi-LAT Observations

2.1 Fermi-LAT Instrument

The Large Area Telescope (LAT) is a pair-conversion γ -ray telescope on board the *Fermi* satellite covering the energy range from about 20 MeV to greater than 300 GeV [8]. The data analyzed here were taken in survey mode over a time period of ~ 5 months from MJD 56658 to MJD 56802 (2014 January 01-May 25). We performed an unbinned likelihood analysis of the data set using the *Fermi*-LAT ScienceTools software package, version v9r32p5¹. Events in a

¹<http://www.fermi.gsfc.nasa.gov/>

circular region of interest (ROI) of radius 10° , centered on the position of B2 1215+30 (R.A. = $12^{\text{h}}17^{\text{m}}52^{\text{s}}$, decl. = $+30^\circ07'00''$, J2000), and with energy $100 \text{ MeV} < E < 100 \text{ GeV}$ were analyzed. In order to avoid contamination by γ -rays from the Earth's limb, additional cuts were applied, accepting only events with a zenith angle $< 100^\circ$ and rocking angle $< 52^\circ$. The background model includes the diffuse emission, all known γ -ray sources from the second *Fermi* catalog within the ROI [9], and the sources that are located up to 5° outside the ROI edges. For modeling the isotropic background and the Galactic diffuse emission, we used the models `iso_source_v05` and `gll_iem_v05` from the *Fermi* Science Tools. We used the set of instrument response functions `P7REP_SOURCE_V15`².

2.2 Lightcurve

To derive the light curve, we performed a standard likelihood analysis with *gtlike*, dividing the data into time bins of three or one day duration. During the fitting procedure, the spectrum of B2 1215+30 in each bin was modeled with a simple power law: $dN/dE = N_0 (E/E_0)^{-\Gamma}$, where N_0 is the normalization factor at a chosen reference energy E_0 , and Γ is the photon index. For all the sources within the ROI detected with a test statistic value of $TS \geq 9$, only the integral flux was left free while the spectral index was fixed to the value obtained during the fitting procedure for the entire time range. For the other sources inside the ROI, detected with a $TS < 9$, all the parameters were frozen to the values obtained during the fitting procedure over the whole time period.

Over the full time period covered by the data set the source was detected with a test statistic value of $TS = 713.9$, corresponding to a detection significance of approximately 26.6σ . Figure 1 shows the counts map of the detected events in a region of size $20^\circ \times 20^\circ$ around B2 1215+30. The 3-day-binned light curve is presented in the bottom panel of Figure 2 and the results are summarized in Table 1. The source exhibits clear variations in flux throughout the observations, curve with a large flare starting on MJD 56693 (2014 February 05). The χ^2 value for a constant flux is $\chi^2/NDF = 219/46$.

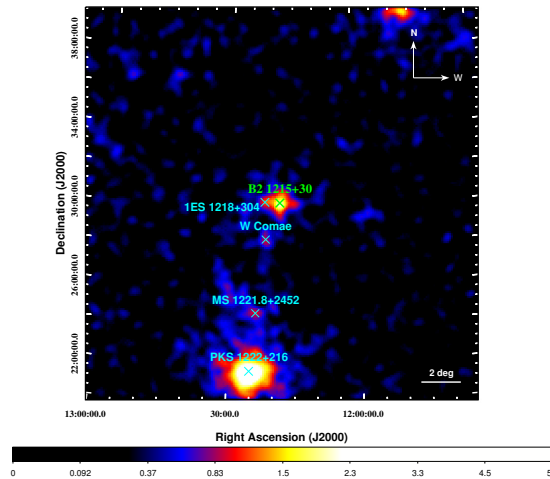


Figure 1: *Fermi*-LAT counts map ($100 \text{ MeV} < E < 100 \text{ GeV}$) produced with a ROI of $20^\circ \times 20^\circ$ centered on the position of B2 1215+30 and selecting only events coming from this region.

²<http://fermi.gsfc.nasa.gov/ssc/data/analysis/user/>

2.3 Spectrum

A spectral analysis was performed on B2 1215+30 in the energy range (0.1-100 GeV) covering the same time period mentioned above. The spectral points were produced by performing the standard unbinned maximum likelihood analysis in 8 energy bands, equally spaced on a logarithmic scale. Similar to the procedure used when fitting the light curve bins, all parameters of the sources in the model of the ROI with $TS < 9$ were fixed during fitting. For the remaining sources in the model with $TS > 9$, only the integral flux was left free, while the spectral index was fixed at the value obtained during the fit for the whole energy range. Figure 3 shows the flux in each energy band plotted with the best-fit power law model over the whole energy range. Upper limits were calculated when the source was detected with $TS < 4$. The best-fit power law model fit gave a spectral index of $\Gamma = 1.84 \pm 0.06$ at a normalization of $N_0 = (6.89 \pm 0.56) \times 10^{-12} \text{ ph cm}^{-2} \text{ s}^{-1} \text{ MeV}^{-1}$.

3. VERITAS Observations

VERITAS (Very Energetic Radiation Imaging Telescope Array System) is an array of four imaging atmospheric-Cherenkov telescopes (IACTs) located at the Fred Lawrence Whipple Observatory in southern Arizona. It detects Cherenkov radiation from energetic particles, produced by the interaction of γ -ray primaries in the atmosphere, using large optical reflectors on the ground

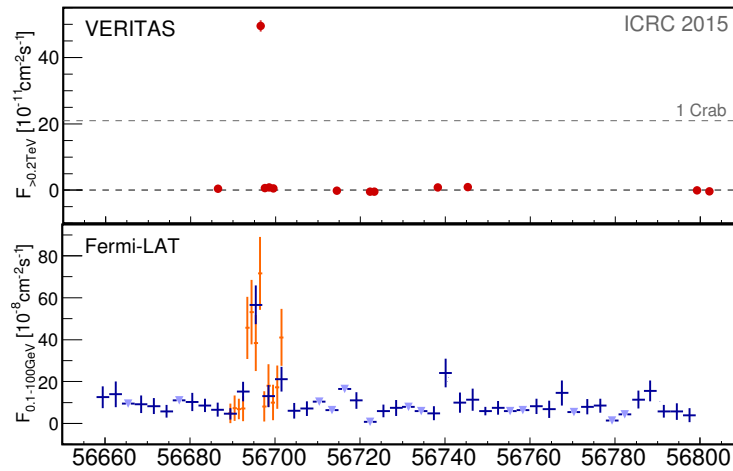


Figure 2: Light curves of B2 1215+30 covering three decades in energy. Top panel: VERITAS ($E > 200$ GeV) light curve in 1-day time bins. Bottom panel: Fermi-LAT ($100 \text{ MeV} < E < 100 \text{ GeV}$) light curve showing the integral flux between 0.1 and 100 GeV in 3-day bins (blue points) and 1-day bins (orange points). The horizontal error bars indicate the duration of the time intervals. Upper limits are shown as downward arrows for a detection significance of less than 2σ .

Table 1: Observations of B2 1215+30

Instrument	Energy range	Dates	Exposure	Signal	Flux [$\text{cm}^{-2} \text{ s}^{-1}$]
VERITAS	$> 0.2 \text{ TeV}$	2014 Jan 29 – May 25	748 min	23.6σ	$(2.4 \pm 0.2) \times 10^{-11}$
Fermi-LAT	$0.1\text{--}100 \text{ GeV}$	2014 Jan 01 – May 25	–	26.6σ	$(8.2 \pm 1.0) \times 10^{-8}$

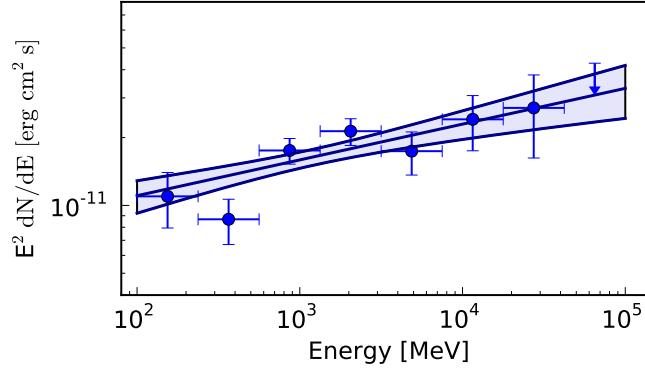


Figure 3: Spectrum of B2 1215+30 as measured by the *Fermi*-LAT between 2014 January 01 and May 25. The solid black line correspond to the best-fit power law. The arrow represents the upper limit calculated for $TS \leq 4$.

[10]. VERITAS is sensitive to γ -rays in the energy range 0.1 and 30 TeV. For these observations of B2 1215+30, data were all taken in "wobble" pointing mode [11], considering that another TeV source, 1ES 1218+304, is in the same field of view, offset 0.76° from B2 1215+30 [3]. Standard VERITAS data processing techniques were used for the analysis, as described in [12], [13]. The energy threshold for this analysis was 200 GeV, with a systematic error of 20 %.

The VERITAS observations carried out between MJD 56686 to 56802 (see Table 1) resulted in a detection of γ -ray signal from B2 1215+30 with a statistical significance of 23.6σ . The top panel of Figure 2 shows the light curve in 1-day time bins, with an average flux over the entire data set of $(2.4 \pm 0.2) \times 10^{-11} \text{ cm}^{-2} \text{ s}^{-1}$. With the exception of 2014 February 08, the observed nightly fluxes are comparable to previously-reported yearly-averaged values [2, 3]. On the night of MJD 56696 (2014 February 08) VERITAS measured a γ -ray flux of $(5.0 \pm 0.2) \times 10^{-10} \text{ cm}^{-2} \text{ s}^{-1}$, which is more than twice that of the Crab Nebula. The source was detected with a statistical significance of 46.5σ in an exposure of 45 minutes. Given the strength of the signal, we derived the light curve in 5-minute time bins (Figure 4). The flux on the night of the flare was more than 60 times brighter than the average flux previously reported by MAGIC and VERITAS from this source [2, 3], making this one of the brightest flares detected in a blazar.

During the night of the flare on 2014 February 08, the atmospheric conditions at the VERITAS site were not optimal, with the presence of a thin layer of high clouds at an altitude of 11 km measured by an onsite ceilometer. Given the energy threshold for this analysis of 200 GeV, it is expected that for γ -ray showers initiated with an energy $E > 200$ GeV, the shower development occurs at altitudes below 11 km. Also the strength of the γ -ray signal (46.6σ) suggests that the cloud layer had little effect on the VERITAS measurement on the night of 2014 February 08. Taking into consideration any effect that a cloud layer could have, the flux reported by VERITAS for this night can be considered a lower limit on the photon flux from B2 1215+30 reaching Earth. Conservatively, we quote no TeV energy spectrum for the bright flare of 2014 February 08.

4. *Swift*-XRT Observations

Following upon the VERITAS detection of the flare, an observation was carried out by the *Swift* mission [14], on 2014-02-09 at 13:31 UT (ObsId 0003190601) with an exposure of 1970

seconds. The photon-counting (PC) mode data were processed with the standard `xrtpipeline` tool (HEASOFT 6.16), with the source and background-extraction regions defined as a 20-pixel (~ 4.7 arcsec) radius circle centered on the source coordinates and a 40-pixel radius circle positioned near the former without overlapping, respectively. The exposure shows a source with a stable average count rate of $\simeq 0.3 \text{ counts s}^{-1}$. Given the low count rate, no pile-up is expected in PC mode, which is confirmed by the acceptable fit of a King profile to the PSF of all observations [15].

Spectral fitting was performed with PyXspec v1.0.4 [16], using dedicated Ancillary Response Functions (ARFs) for the XRT data set generated by `xrtmkarf` (along with the latest spectral redistribution matrices `swxpc0t012s6_20110101v014` from CALDB). The spectrum was rebinned to have at least 20 counts per bin using `grppha`, and channels 0 to 29 were ignored in the XRT-PC data. The data were fit to a power-law model $dN/dE = N_0(E/E_0)^{-\Gamma_X}$. Using the Leiden/Argentine/Bonn (LAB) Survey of Galactic HI weighted average hydrogen column density, a value of $N_H = 1.68 \times 10^{20} \text{ cm}^{-2}$ was used, and a good fit was obtained for the power-law function ($P(\chi^2) = 0.42$) with a photon index of $\Gamma_X = 2.54 \pm 0.07$. The unabsorbed 0.3 – 10 keV flux was found to be $F_{0.3-10\text{keV}} = 1.28 \text{ erg cm}^{-2} \text{ s}^{-1}$, retrieved using `cflux`. A fit to a log-parabolic model with one more parameter compared to the power-law model gives an improved fit ($P(\chi^2) = 0.42$) but an F-test gives a high probability of 10% that this is due to chance only.

5. Doppler factor estimation

5.1 Variability time scale

In order to further investigate the flare, we binned the *Fermi*-LAT integral fluxes into 1-day observations for a shorter time range MJD 56689-56703 (2014 February 01-15), centered on the flare period. From the 1-day light curve we evaluated the variability time scale, defined here as the time in which the flux increases by a factor of two, with an exponential function of the form:

$$F(t) = F_C + F_0 \cdot 2^{(t-t_0)/t_{\text{var}}}, \quad (5.1)$$

where F_C is a constant fit to the average flux of the source, F_0 is the flux at the instant of the flare at t_0 , and t_{var} is the variability time scale. From the fit, the variability time scale is estimated to be $t_{\text{var}} = (0.188 \pm 0.09)$ days (blue dashed line in Figure 4). We also fitted the full 1-day binned light curve with the function given in Equation 6 of [17] :

$$F(t) = F_C + F_0 \left[\exp\left(\frac{t_0 - t}{t_r}\right) + \exp\left(\frac{t - t_0}{t_d}\right) \right]^{-1} \quad (5.2)$$

This gives a rise time of $t_r = (0.184 \pm 0.25)$ days, consistent with our exponential fit (green dashed line in Figure 4).

5.2 Doppler factor calculation

For a power-law spectrum of index -3.0 , the flux above 0.2 TeV as measured by VERITAS during the flare corresponds to an isotropic luminosity of $1.5 \times 10^{46} \text{ erg s}^{-1}$. Assuming a spherical emission region of radius R , the variability time scale derived from the *Fermi*-LAT light curve constrains the size of the emission region to be $R\delta^{-1} \leq ct_{\text{var}}/(1+z) \leq 4.3 \times 10^{14} \text{ cm}$. It is expected that this high luminosity emitted in such a compact volume will result in strong photon-photon absorption, resulting in lower-energy photons. However, since we observe high-energy

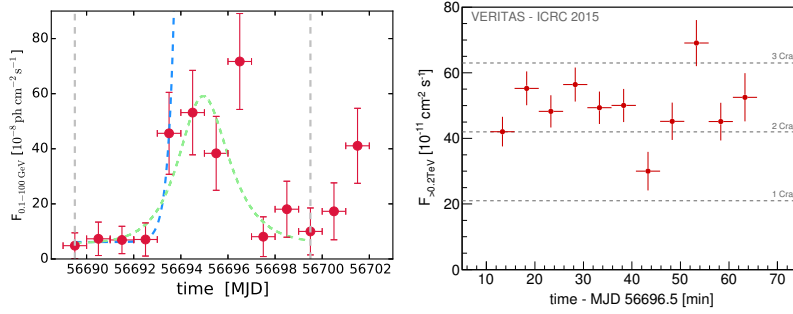


Figure 4: Light curve of B2 1215+30 during the flare. Left plot: *Fermi*-LAT light curve showing the averaged integral flux in bins of 1-day duration, from MJD 56689 to MJD 56703. The blue and green lines show the fits to the data (see text). The data points between the gray dashed lines were included in the fit. Right plot: VERITAS light curve of B2 1215+30 on the night of the flare (MJD 56696). Photon fluxes are calculated in 5-minute bins. A fit of the data points to a constant flux yields χ^2/NDF of 25.68/10 corresponding to a p-value of $P = 4.2 \times 10^{-3}$.

γ -ray emission, the emitting region must be transparent to γ -rays ($\tau_{\gamma\gamma} \leq 1$). If the high-energy γ -rays are emitted from a region that is co-located with the X-rays then we might expect attenuation due to photon-photon absorption.

Assuming that X-rays and γ -rays observed with the *Swift*-XRT and the *Fermi*-LAT are produced in a single region of the source object, the opacity implies a minimum Doppler factor such that the rest frame density of low-energy radiation is sufficiently small that the γ -rays can escape. Following the argument described in [18], the minimum Doppler factor is given by the expression

$$\delta \geq \left[\frac{\sigma_T d_L^2 (1+z)^{2\alpha} F_{1\text{keV}}}{5hc^2 t_{\text{var}}} \left(\frac{E_\gamma}{\text{GeV}} \right)^\alpha \right]^{\frac{1}{(4+2\alpha)}} \quad (5.3)$$

where σ_T is the Thomson cross section, d_L the luminosity distance, α the X-ray spectral index, E_γ the highest energy photon and $F_{1\text{keV}}$ the X-ray flux measured in μJy .

We used *gtselect* from the *Fermi* ScienceTools to find the highest energy photon from B2 1215+30 at GeV energies, accepting only photons within 1° of the center of ROI within the energy limits chosen for this analysis, for the time period of the flare. From this analysis the highest energy photon was found to be to be $E_{\text{max}} = 73.6$ GeV. The density of low energy photons was derived from contemporaneous observations at X-ray energies carried out with *Swift*. Using the pair-production argument as described in [18], the minimum Doppler is estimated to be $\delta \geq 5.7$, consistent with what is seen with the TeV blazars [19].

6. Summary and Conclusions

VERITAS and *Fermi*-LAT observed a bright γ -ray flare from the BL Lac object B2 1215+30 on 2014 February 08, equivalent with 200 % of the Crab Nebula flux (a standard measure in γ -ray astronomy). At GeV energies the flare starts on 2014 February 05, whereas at TeV energies the flare was seen by VERITAS on 2014 February 08. The variability time scale of the source was derived from the *Fermi*-LAT light curve to be $t_{\text{var}} \simeq 4.5\text{h}$. Using the opacity argument and following the calculation of [18] we derived the minimum Doppler factor to be $\delta \geq 5.7$, consistent with what we see in TeV blazars [19].

VERITAS research is supported by grants from the U.S. Department of Energy of Science, the U.S. National Science Foundation and the Smithsonian Institution, by NSERC in Canada, and by Science Foundation Ireland (SFI 10/RFP/AST2748). We acknowledge the

excellent work of the technical support at the Fred Lawrence Whipple Observatory and at the collaborating institutions in the construction and operation of the instrument. The VERITAS Collaboration is grateful to Trevor Weekes for his seminal contributions and leadership in the field of VHE γ -ray astrophysics, which made this study possible. RM gratefully acknowledges support from the Alliance Program at Ecole Polytechnic and Columbia University.

References

- [1] G. Colla et al., *A catalogue of 3235 radio sources at 408 MHz*, A&AS (1970) 281.
- [2] J. Aleksić et al., *Discovery of VHE γ -rays from the blazar 1ES 1215+303 with the MAGIC telescopes and simultaneous multi-wavelength observations*, A&A (2012) [[arXiv:1203.0490](#)].
- [3] E. Aliu et al., *Long Term Observations of B2 1215+30 with VERITAS*, ApJ (2013) [[arXiv:1310.6498](#)].
- [4] E. Nieppola et al., *VizieR Online Data Catalog: SED of BL Lacertae objects*, VizieR Online Data Catalog (2006) 50441.
- [5] M. Akiyama et al., *Optical Identification of the ASCA Medium Sensitivity Survey in the Northern Sky: Nature of Hard X-Ray-Selected Luminous Active Galactic Nuclei*, ApJS (2003) [[astro-ph/0307164](#)].
- [6] K. M. Lanzetta et al., *Ultraviolet spectra of QSOs, BL Lacertae objects, and Seyfert galaxies*, ApJS (1993).
- [7] C. M. Urry and P. Padovani, *Unified Schemes for Radio-Loud Active Galactic Nuclei*, PASP (1995) [[astro-ph/9506063](#)].
- [8] W. B. Atwood et al., *The Large Area Telescope on the Fermi Gamma-Ray Space Telescope Mission*, ApJ (2009) [[arXiv:0902.1089](#)].
- [9] P. L. Nolan et al., *VizieR Online Data Catalog: Fermi LAT second source catalog*, VizieR Online Data Catalog (2012).
- [10] J. Holder, *VERITAS: Status and Highlights*, ICRC (2011) [[arXiv:1111.1225](#)].
- [11] V. P. Fomin et al., *New methods of atmospheric Cherenkov imaging for gamma-ray astronomy. I. The false source method*, Astroparticle Physics (1994).
- [12] V. A. Acciari et al., *Veritas Observations of a Very High Energy γ -Ray Flare From the Blazar 3C 66A*, ApJ (2009) [[arXiv:0901.4527](#)].
- [13] S. Archambault et al., *Discovery of a New TeV Gamma-Ray Source: VER J0521+211*, ApJ (2013) [[arXiv:1308.5017](#)].
- [14] D. N. Burrows et al., *The Swift X-Ray Telescope*, Space Sci. Rev. (2005) [[astro-ph/0508071](#)].
- [15] A. Moretti et al., *In-flight calibration of the Swift XRT Point Spread Function*, in Gamma-Ray Bursts in the Swift Era (S. S. Holt, N. Gehrels, and J. A. Nousek, eds.), vol. 836 of American Institute of Physics Conference Series, 2006.
- [16] K. A. Arnaud, *XSPEC: The First Ten Years*, in Astronomical Data Analysis Software and Systems V, Astronomical Society of the Pacific Conference Series, 1996.
- [17] A. A. Abdo et al., *Gamma-ray Light Curves and Variability of Bright Fermi-detected Blazars*, ApJ (2010) [[arXiv:1004.0348](#)].
- [18] L. Dondi and G. Ghisellini, *Gamma-ray-loud blazars and beaming*, MNRAS (1995).
- [19] B. Rani et al., *Constraining the location of rapid gamma-ray flares in the flat spectrum radio quasar 3C 273*, A&A (2013) [[arXiv:1307.0854](#)].